



**HAL**  
open science

## Fluorination effect on the solubility of C60 in a bis(trifluoromethylsulfonyl)imide based ionic liquid

Yasser Ahmad, Jean-Michel Andanson, Pierre Bonnet, Nicolas Batische, Daniel Claves, Marc Dubois, Agílio Pádua

### ► To cite this version:

Yasser Ahmad, Jean-Michel Andanson, Pierre Bonnet, Nicolas Batische, Daniel Claves, et al.. Fluorination effect on the solubility of C60 in a bis(trifluoromethylsulfonyl)imide based ionic liquid. *Colloids and Surfaces A: Physicochemical and Engineering Aspects*, 2022, 649, pp.129140. 10.1016/j.colsurfa.2022.129140 . hal-03702400

HAL Id: hal-03702400

<https://uca.hal.science/hal-03702400v1>

Submitted on 7 Nov 2022

**HAL** is a multi-disciplinary open access archive for the deposit and dissemination of scientific research documents, whether they are published or not. The documents may come from teaching and research institutions in France or abroad, or from public or private research centers.

L'archive ouverte pluridisciplinaire **HAL**, est destinée au dépôt et à la diffusion de documents scientifiques de niveau recherche, publiés ou non, émanant des établissements d'enseignement et de recherche français ou étrangers, des laboratoires publics ou privés.



Distributed under a Creative Commons Attribution - NonCommercial - NoDerivatives 4.0 International License

# Fluorination effect on the solubility of C<sub>60</sub> in a bis(trifluoromethylsulfonyl)imide based ionic liquid

Yasser Ahmad<sup>a</sup>, Jean-Michel Andanson<sup>\*b</sup>, Pierre Bonnet<sup>\*b</sup>, Nicolas Batisse<sup>b</sup>, Daniel Claves<sup>b</sup>, Marc Dubois<sup>b</sup>, Agilio Padua<sup>b,†</sup>

<sup>a</sup>*Fahad Bin Sultan University, College of Sciences and Humanities, Department of Natural Sciences, P.O. Box 15700, Tabuk 71454, Kingdom of Saudi Arabia*

<sup>b</sup>*Université Clermont Auvergne, CNRS, SIGMA Clermont, Institut de Chimie de Clermont-Ferrand, F-63000 Clermont-Ferrand, France.*

<sup>†</sup>*Present address : Laboratoire de Chimie de l'ENS Lyon, CNRS and Université de Lyon, 46 allée d'Italie, 69364 Lyon, France.*

## Abstract

Highly fluorinated fullerenes with a chemical composition of C<sub>60</sub>F<sub>48</sub> have been prepared and characterized. Their solubility of the new nanomaterials in the ionic liquid (IL) has been compared with raw fullerenes C<sub>60</sub>. Fluorination may appear as a convenient method to enhance the solubility of carbonaceous nanomaterials in a fluorinated based anion IL. Indeed, the ability of 1-butyl-3-methylimidazolium bis(trifluoromethylsulfonyl)imide ([BmIm][NTf<sub>2</sub>]), to solubilize C<sub>60</sub> and C<sub>60</sub>F<sub>48</sub> was investigated using optical microscopy and UV-vis spectroscopy. While C<sub>60</sub> has very poor solubility in this IL (below 0.07 mmol/L), the solubility increases at least eightfold, i.e. more than 1.0 mg/mL (or 0.61 mmol/L) for C<sub>60</sub>F<sub>48</sub> samples. The presence of fluorine atoms on fullerene seems to enhance the stability of the solvated molecules in IL thanks to the limitation of the aggregation of C<sub>60</sub>F<sub>48</sub> in [BmIm][NTf<sub>2</sub>]. This improvement of the solubility could be explained by the beneficial effect of the fluorination that induces a decrease of the  $\pi$ - $\pi$  interaction between carbonaceous solutes as the carbon hybridization changes from sp<sup>2</sup> to sp<sup>3</sup> through the formation of C-F covalent bonds and thus enhances the interaction between the solvent and the solute. Fluorination appears as an efficient approach to limit the use of volatile organic compounds usually used as co-solvent to enhance the dispersion mechanism.

Keywords: C<sub>60</sub> fullerenes, fluorinated fullerenes, ionic liquids, solubility.

\* Corresponding author

## 1. Introduction

Suspensions of colloidal  $C_{60}$  particles have attracted attention because of their biological and antioxidant activities, nanotoxicity, and unusual photochemical properties [1-6]. The industrial production of  $C_{60}$  is widespread in areas such as drug delivery and energy conversion systems [7]. Moreover, many of the chemical and physical processes involving carbonaceous nanomaterials could benefit from solution-phase methods for synthesis, preparation, purification, or transfer onto substrates.

The solubility/dispersibility of fullerenes among other carbonaceous materials (like graphene [8] ) is both of practical and fundamental interest. In particular, solubility in the organic solvent has been extensively studied [9-11]. Over 150 solvents have been so far probed to disperse fullerenes, with quite moderate success. For example, Ruoff et al.[9] have studied the room temperature solubility of pure  $C_{60}$  as a function of solvent properties (such as index of refraction, dielectric constant, H-bonding character, and molecular size) in 47 organic solvents. The solubility covers a wide range from 0.01 mg/mL in methanol to 50 mg/mL in 1-chloronaphthalene. The authors showed also that the H-bonding character of the solvent is a discriminating factor.  $C_{60}$  has a lower solubility in solvents that organize themselves through polar or H-bond interactions. The solvation of non-polar  $C_{60}$ , which does not participate in H-bonds, leads to the unfavorable disruption in the solvent assembly [9]. The highest solubility of  $C_{60}$  was achieved by Talukdar et al.[12], who used piperidine (reaching in 53 mg/mL concentration) and pyrrolidine (48 mg/mL). It was hypothesized that these solvents exhibited specific donor-acceptor interactions with  $C_{60}$ ,  $C_{70}$ ,  $C_{84}$ ,  $C_{100}$  that may, under certain conditions, result in the formation of new chemical compounds.  $C_{60}$  solvation in the imidazolium-based ionic liquid (IL) was mainly studied by theoretical investigations [3, 5, 6, 13, 14, 15]. Despite the importance of these computational works, few experimental works have been performed in this field. For example, Pamies et al. prepared few-layers graphene dispersed an ionic liquid (IL) by mechanical mixing and sonication. The obtained graphene dispersions showed an interesting tribological performance as they are able to reduce wear rates in sapphire-steel sliding contacts, which prevent surface damage [8].

This work investigates the experimental effect of the functionalization by fluorination on the solvation of fullerene in an imidazolium-based ionic liquid.

Room-temperature ionic liquids (RTILs) may constitute universal solvents [16], whereas solvation of fullerenes is notoriously problematic due to their exclusive structure and interaction behavior[2-6]. If efficient solvents for fullerenes are found, their applications

would be heavily increased. The use of ILs as innovative solvents is rising significantly mainly because of their negligible volatility. This characteristic makes them promising replacements to volatile organic compounds (VOCs), which are a source of major environmental problems.

In this work, the solvation of fullerenes and fluorinated fullerenes in room temperature ionic liquid was investigated. As a matter of fact, reaction with molecular fluorine  $F_2$  gas or other fluorinating agent ( $XeF_2$  [13],  $KrF_2$  [17],  $TbF_4$  [18],  $CeF_4$  or  $K_2PtF_6$  [19]) drastically changes the electronic properties and surface chemistry [19, 20] of the carbonaceous materials. Moreover, the carbon hybridization changes from  $sp^2$  to  $sp^3$  with the formation of a covalent C-F bond;  $\pi$ - $\pi$  interaction between fullerenes is then suppressed. Moreover, electrostatic repulsion between fluorine atoms is expected. In such a way, the effect of fluorination on the ILs/ $C_{60}$  interaction was investigated. Because of their well-defined size and spherical geometry,  $C_{60}$  appears as a model compound for the investigation of interaction with ILs before extrapolation to other  $sp^2$  containing carbonaceous materials with 1D or 2D dimensionality, i.e. nanotubes and graphene.

Due to a large number of addition sites, the reaction of fluorine gas or fluorinating agent with  $C_{60}$  fullerene leads to a wide composition range, from  $C_{60}F_2$  to  $C_{60}F_{60}$ . Owing to the steric hindrance that occurs at the surface of the molecule during the fluorine addition, fluorofullerene with a composition of  $C_{60}F_{48}$  is considered as the compound with maximum fluorine content that can be synthesized in pure form through direct fluorination using pure molecular fluorine [2, 3, 5, 6, 13, 17-19]. As  $C_{60}F_{48}$  exhibits a spherical geometry contrary to the other compositions with less fluorine, it appears as a model compound. The relative amount of  $C_{60}F_{48}$  among other compositions strongly depends on the fluorination temperature and its duration. Using both fluorine gas and a fluorinating agent, thermally induced disruption of the fullerene skeleton can occur above  $350^\circ C$  resulting in the formation of  $C_{60}F_x$  ( $x > 60$ ) species (hyperfluorination). In the present study, the highest fluorination rate, fluorination conditions may be strengthened to reach this stage resulting in a nearly pure  $C_{60}F_{48}$  compound. A minute control of the fluorination conditions is then necessary both to avoid the decomposition and to increase the relative content of  $C_{60}F_{48}$ .

## 2. Experimental

### 2.1. Synthesis

1-Butyl-3-methylimidazolium bis(trifluoromethylsulfonyl)imide([BmIm][Ntf<sub>2</sub>]) with a purity of higher than 99% was purchased from IoLiTec (Ionic Liquids Technologies GmbH). Before use, IL was dried at room temperature under a vacuum (0.1 mbar) for around 24 hours.

Fluorination was carried out under pure F<sub>2</sub> gas flow in a nickel reactor heated with a regulated furnace. The starting material was placed in a monel boat. The starting materials are commercial products from Sigma Aldrich (99.5%). Prior to reaction, C<sub>60</sub> was dehydrated and rid of solvent under dynamic vacuum (obtained with a primary pump) at 180 °C for 20 hours. Because perfluorofullerenes are known to be unstable at high temperatures, the reaction at those conditions must be curtailed before weight uptake falls off. So, a drastic control of the conditions was performed according to the duration, the temperature, pure fluorine flow, and the initial weight to avoid the decomposition of carbon. The most fluorinated compound was obtained using 100 mg of C<sub>60</sub> for 4 h at 300 °C giving a white color powder. The increase of the fluorine content results in the depletion of the  $\pi/\pi^*$  states and the increase of the HOMO–LUMO gap, as for isolated fluorofullerene molecules, and therefore reduced the opportunity of an electronic transition occurrence in the visible range [17, 18]. The increase of the fluorine content then leads to a progressive transition of the microcrystalline fluorofullerene powders toward the white color. Thus, over the C<sub>60</sub>F<sub>n</sub> series with n = 2, 8, 18, 20, 36, and 48, the brown, red, yellow-green, off-white, cream-white, and white colors were distinctly observed [21, 22]. The white color obtained in the present work is the first indication of highly fluorinated C<sub>60</sub>. Because decomposition under fluorine gas may occur with the release of fluorocarbon gaseous species such as CF<sub>4</sub> and C<sub>2</sub>F<sub>6</sub> (and then loss of carbon), the weight uptake is not suitable for the estimation of the fluorine content. Additional characterization such as solid-state NMR is necessary to determine a more accurate composition. Several syntheses of C<sub>60</sub>F<sub>48</sub> were performed in the same condition to provide sufficient quantities for dispersion tests. All products issued were identical in terms of appearance (white powder) and physical-chemical properties (see section 2.2).

## 2.2 Physical-chemical characterization of the powders

X-ray diffraction powder (XRD) patterns were obtained using a Philips diffractometer with a Cu(K<sub>α</sub>) radiation ( $\lambda = 0.15406$  nm).

NMR experiments were performed at room temperature using a Bruker Avance spectrometer (working frequencies for <sup>13</sup>C and <sup>19</sup>F were equal to 73.4 and 282.2 MHz, respectively). A magic angle spinning (MAS) NMR probe (Bruker) working with a 4 or 2.5 mm rotor was

used. For  $^{19}\text{F}$  MAS spectra, a simple sequence was used with a single  $\pi/2$  pulse duration of 5.5  $\mu\text{s}$ . The  $^{13}\text{C}$  spectra were recorded using a solid echo sequence (two 5.5  $\mu\text{s}$   $\pi/2$  pulses separated by 25  $\mu\text{s}$ ); this sequence allows the acquisition of the whole signal without loss due to the electronic dead time followed by a quantitative determination of the different contributions. The recycle times were equal to 3 s for  $^{19}\text{F}$  and 20 s for  $^{13}\text{C}$  spectra. The scan numbers were 256 and 4000 for  $^{19}\text{F}$  and  $^{13}\text{C}$  measurements, respectively.  $^{19}\text{F}$  and  $^{13}\text{C}$  chemical shifts were referenced to  $\text{CFCl}_3$  and tetramethylsilane (TMS), respectively.

### **2.3 Physical-chemical characterization of the liquid phases**

To ensure good solubilization and avoid clusters of fullerene-based compounds, the suspensions of  $\text{C}_{60}$  and  $\text{C}_{60}\text{F}_{48}$  in  $[\text{BmIm}][\text{NTf}_2]$  have been prepared by first dissolving the powders in dichloromethane at a concentration of 0.2 mg/ml for  $\text{C}_{60}$  and 1 mg/ml for  $\text{C}_{60}\text{F}_{48}$  (sonication for 1 hour at room temperature, Branson 5800). An adequate amount of one of these solutions was added to 3 ml of IL. After a homogeneous solution was obtained, the volatile solvent has been evaporated slowly under ambient conditions. Traces of volatiles were then removed under vacuum at 0.1 mbar for a couple of hours at room temperature. The IL with a well-known amount of  $\text{C}_{60}$  or  $\text{C}_{60}\text{F}_{48}$  was then transferred into a UV-vis cuvette for spectroscopic measurements. Each cuvette was sealed and conserved in the dark at 20°C between measurements. UV-vis spectra were recorded regularly for weeks to follow the sedimentation of the particles in the viscous IL. The neat IL conserved in the same conditions was used to record the background of all UV-vis spectra. The IL used in this work is strongly absorbing below 260 nm, restraining our UV-vis analysis to the range between 260 and 600 nm.

UV-vis spectrometer was a Jasco V-650 and solution was placed in QS cuvettes from Hellma with a path length of 10 mm.

Pictures of the bottom of the cuvette were taken using a portable microscope to observe the sedimentation. The microscope (digital microscope AM7915MZT from Dino-lite) has been placed under the cuvette to observe the bottom of each cuvette (magnification x180).

## **3. Results and discussions**

### **3.1 Fluorination of $\text{C}_{60}$ fullerene**

The obtained fluorinated compound has a white color ( $\text{C}_{60}\text{F}_{48}$ ) in contrast with the black precursor ( $\text{C}_{60}$ ). The structural change of  $\text{C}_{60}$  during fluorination is demonstrated with the X-

ray diffractograms (Fig.1-a). The disappearance of all the characteristic peaks of raw  $C_{60}$  is observed meaning the completion of the fluorination. Pure  $C_{60}$  belongs to the  $Fm\bar{3}m$  space group and is characterized by a parameter  $a = 1.417$  nm for the f.c.c. lattice. The value of this parameter is sometimes reported with a small divergence from that given above (e.g. 1.4198 nm [23]) but it might be due to residual solvent, moisture, or  $C_{70}$  traces.

The XRD pattern of the highly-crystallized  $C_{60}$  fluorinated at 300 °C can no longer be indexed by a cubic lattice and an I-centered tetragonal (bct) cell was used [24]. The lattice parameters are  $a = 1.675$ nm and  $c = 1.790$  nm due to the fluorine accommodation through the molecule. Indeed, the addition of fluorine atoms increases the size of the  $C_{60}$  and also creates an electrostatic repulsion, both inducing an increase of the lattice parameter. The diffractogram of the fluorinated compound is in good agreement with the expected diffractogram for the compound  $C_{60}F_{48}$  as reported in the literature [24]. It shows that non-fluorinated  $C_{60}$  molecules remain and that the applied fluorination conditions have made it possible to exceed the stoichiometry  $C_{60}F_{36}$  [24].

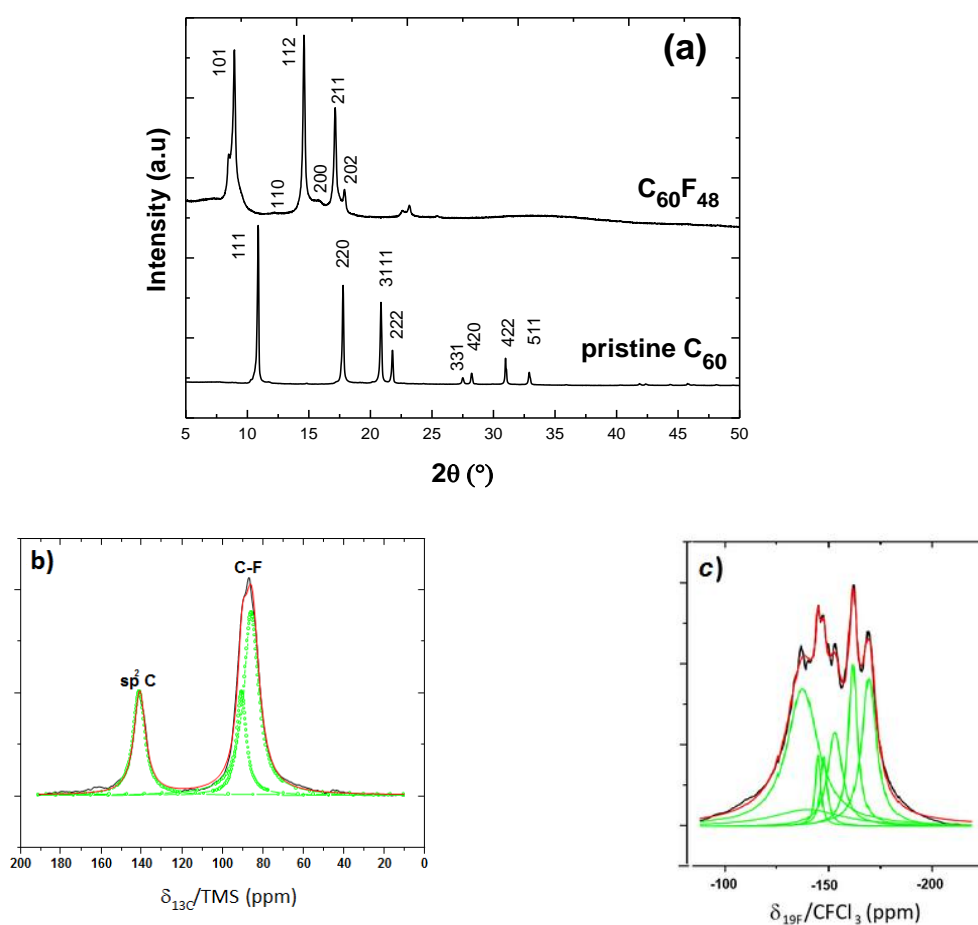


Fig. 1. (a) X Ray diffractograms of  $C_{60}$  and  $C_{60}F_{48}$ .



(b)  $^{13}\text{C}$  and (c)  $^{19}\text{F}$  MAS NMR spectra of  $\text{C}_{60}\text{F}_{48}$  (at 10 kHz and 30 KHz, respectively)

Solid-state NMR with  $^{13}\text{C}$  and  $^{19}\text{F}$  nuclei (Fig.1-b and Fig.1-c, respectively) also evidence the existence of several C-F covalent bonds in fluorinated  $\text{C}_{60}$  because of several grafting sites of fluorine atoms onto a carbon involved in either a hexagon or pentagon cycles. Moreover, the presence of non-fluorinated carbon ( $\text{sp}^2\text{C}$ ) acts also on the C-F bonding because of the interaction with neighboring C-F bonds (hyperconjugation) [25]. Non-fluorinated  $\text{sp}^2$  carbon atoms are highlighted by the presence of a peak at 140ppm in addition to the main peak at 88ppm on the  $^{13}\text{C}$  spectrum. The latter peak is characteristic of the covalent C-F bonds [26-30]. Two components (Lorentzian) are necessary to fit the C-F lines corresponding to the presence of two sets of C-F bonds. The fluorine content, i.e. the atomic F/C ratio, is extracted from the fit of the  $^{13}\text{C}$  spectrum (Fig. 1-b).  $F/C = (S1_{\text{C-F}} + S2_{\text{C-F}}) / (S1_{\text{C-F}} + S2_{\text{C-F}} + S_{\text{Csp}^2})$  where  $S1_{\text{C-F}}$  and  $S2_{\text{C-F}}$  are the integrated area of the two lines for C-F bonds,  $S_{\text{Csp}^2}$  being the line of non-fluorinated carbon atoms. F/C is found equal to 0.78 with an accuracy of 0.02 meaning a  $\text{C}_{60}\text{F}_{48}$  composition (F/C=0.8) or very close. Thus NMR results are in very good agreement with the XRD pattern in Fig. 1-a.

At least eight contributions of covalent C-F bonds are evidenced by  $^{19}\text{F}$  NMR (with a MAS rate of 30 kHz) by the multitude of lines observed between -120 and -200 ppm vs  $\text{CFCl}_3$  (Fig.1-c). The origin of these lines was discussed previously [23]. It is to note the absence of narrow lines at -120 and 110 ppm on the  $^{19}\text{F}$  and  $^{13}\text{C}$  spectra, respectively, that are assigned to  $\text{CF}_2$  groups. This is the evidence that broken  $\text{C}_{60}$  cages are not present in the sample because of the decomposition during the fluorination, so the integrity of the closed carbonaceous skeleton is preserved. In conclusion, the main product obtained after fluorination exhibits a composition of  $\text{C}_{60}\text{F}_{48}$  with high purity as evidenced by NMR and XRD. This sample was used to prepare the solution in fluorine-containing RTILs.

### 3.2 Reactivity between $\text{C}_{60}\text{F}_{48}$ and IL

The IL used as a solvent may also be reactive against  $\text{C}_{60}\text{F}_{48}$ . To better understand the interaction between ILs and  $\text{C}_{60}\text{F}_{48}$ ,  $^{19}\text{F}$  NMR spectrum of the  $\text{C}_{60}\text{F}_{48}$  dispersion in IL (3 mg/mL concentration and after storage for 6 weeks) was recorded and compared to the spectra of the solvent and solute (powder without MAS) (Fig.2). The narrow line at -78.5 ppm is unambiguously assigned to  $\text{CF}_3$  groups of the  $[\text{NTf}_2]$  anion. Magnification in the -100/-200 ppm range evidence the presence of  $\text{C}_{60}\text{F}_{48}$  molecules in the dispersion. Two differences appear in comparison with the powder. Firstly, the broadness of the superimposed bands (related to the presence of C-F bonds with different covalences) is significantly lower for

solvated  $C_{60}F_{48}$  (full width at half maximum f.w.h.m. of 8.5 kHz) than for the molecules in the crystalline powder (f.w.h.m. = 11.8 kHz); IL decreases the  $^{19}F$ - $^{19}F$  homonuclear dipolar coupling by separation of the  $C_{60}F_{48}$  molecules. Secondly, an additional narrow line with weak intensity is observed at -152 ppm on the spectrum of the  $C_{60}F_{48}$  dispersion contrary to the powder. A few C-F bonds with the weakest covalence may be broken because of the strong interaction with ILs. In other terms, partial defluorination occurs with the formation of solvated  $F^-$  anions with a chemical shift of -152 ppm. This process could be thermally activated during the sonication. Regarding the integrated area of this band of  $F^-$  and the superimposed bands of  $C_{60}F_{48}$ , only one fluorine atom per 120 is transferred as  $F^-$  into the solvent. The removed fluorine atom is the one with the weakest C-F covalence, i.e. the highest  $^{19}F$  chemical shift (-132 ppm). The reaction results in a composition of  $C_{60}F_{47.5}$ . Such a transfer is too weak to change the optical properties in the visible range. That demonstrates the good chemical stability of  $C_{60}F_{48}$  in [BmIm][NTf<sub>2</sub>].

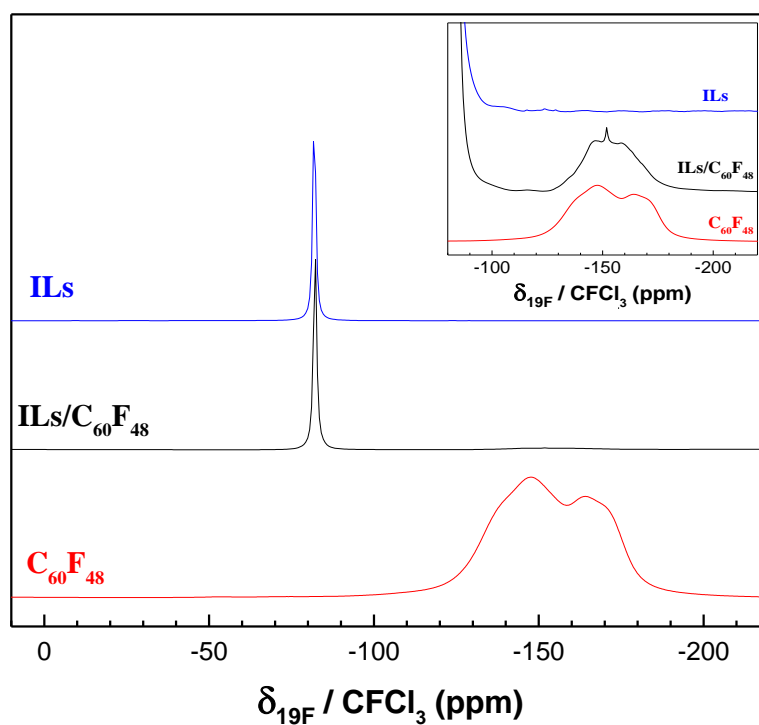
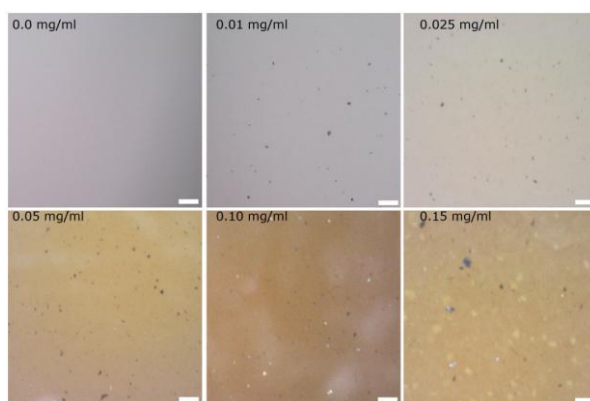


Fig. 2.  $^{19}F$  NMR spectra of the 3 mg/mL  $C_{60}F_{48}$  dispersion, RTILs, and  $C_{60}F_{48}$  powder (without MAS). Insert is a zoom in the range [-80, -220 ppm] for  $C_{60}F_{48}$  dispersion and RTILs and compared with  $C_{60}F_{48}$  powder (without zoom)

### 3.3 Solvation / dispersion tests

To evaluate the stability over long periods of  $C_{60}$  and  $C_{60}F_{48}$  dispersions into [BmIm][NTf<sub>2</sub>], we have studied the ability of IL to conserve isolated fullerene species rather than clusters. In this way, to avoid clusters of  $C_{60}$  and  $C_{60}F_{48}$  in dispersions, each carbon powder was first dissolved in a volatile organic solvent below the solubility of  $C_{60}$  and  $C_{60}F_{48}$ . Then, IL was added and the volatile solvent evaporated slowly. This procedure has been chosen over the direct dissolution of material into the IL to ensure that all  $C_{60}$  (or  $C_{60}F_{48}$ ) has been dissolved at one stage. After the removal of volatiles under a vacuum, the liquid was observed with an optical microscope.

In the case of  $C_{60}$  suspension, the range of concentration studied was up to 0.30 mg/mL. Images of the bottom of the sample after a few hours are shown in Fig.3. The microscopic observation was realized with the microscope placed below the sample and the cuvette was placed to observe the sedimentation: the focus was made on the layer of liquid in contact with the bottom face of the UV-visible cuvette. At all concentrations of  $C_{60}$  from 0.01 to 0.30 mg/mL, agglomerated particles of  $C_{60}$  are observable. The sizes of the observed particles are up to around 50  $\mu\text{m}$ . Even for the lowest concentration studied, at 0.01 mg/mL, agglomerates of  $C_{60}$  are observed. Moreover, the solution became yellowish with the increase of concentration of  $C_{60}$ . This coloration is also clearly observable while looking at the solution with the naked eye (Fig.4).



**Fig. 3. Pictures of samples containing different concentrations (0.0 mg/mL; 0.01 mg/mL; 0.025 mg/mL; 0.05 mg/mL; 0.10 mg/mL; 0.15 mg/mL) of  $C_{60}$  in [BmIm][NTf<sub>2</sub>] just after preparation. Scale bar: 100  $\mu\text{m}$ .**

The samples are sealed and kept in the dark at 20°C for 6 weeks to observe the sedimentation of  $C_{60}$  agglomerates. After preparation, the suspensions with the highest concentrations of  $C_{60}$  are completely opaque while the samples with the lowest concentrations are clear or slightly yellowish. Pictures of  $C_{60}$  in IL after preparation and after 6 weeks of sedimentation are given in Fig.4. After the preparation, as observed with the images obtained with the microscope, coloration appears while increasing the concentration of the  $C_{60}$  in IL. For concentrations

higher than 0.20 mg/mL, the suspension of C<sub>60</sub>/IL is even opaque with the path length of 10 mm of the UV-vis cuvette. While at the lowest concentration of C<sub>60</sub>, the samples are keeping their aspects, at the highest concentration the sedimentation could be observed; for concentration from 0.10 to 0.30 mg/mL, C<sub>60</sub> has agglomerated, and the agglomerates are forming a layer at the bottom of the cuvettes. At the same time, the top parts of the samples are becoming clearer indicating the formation of a supernatant liquid phase and most probably the decrease of the C<sub>60</sub> concentrations in this part of the samples. ILs are viscous, even [BmIm][NTf<sub>2</sub>] which is known to have a moderate viscosity at room temperature around 60 mPa.s [31], and are inducing slow precipitation of C<sub>60</sub>.

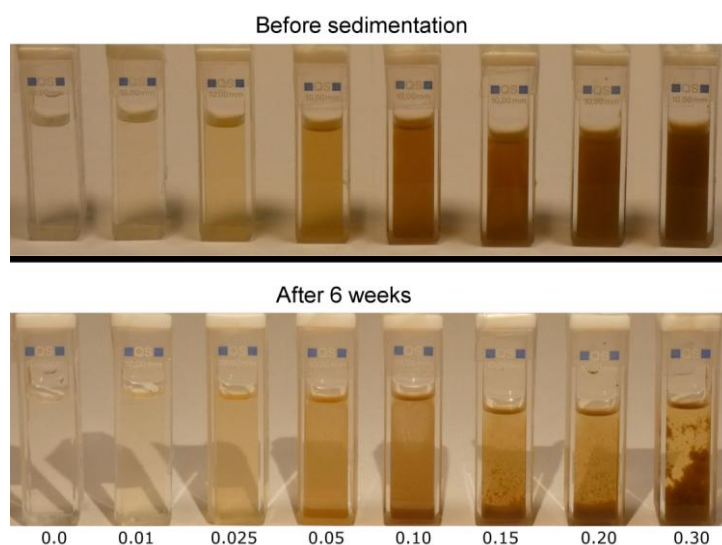


**Fig. 4.** Picture of UV-vis cuvettes containing different amounts of C<sub>60</sub> in [BmIm][NTf<sub>2</sub>] after preparation (top) and after 6 weeks of sedimentation (bottom). The concentrations of C<sub>60</sub> are increasing from left to right, from 0 to 0.30 mg/mL.

Various concentrations, up to 3 mg/mL, of C<sub>60</sub>F<sub>48</sub> in [BmIm][NTf<sub>2</sub>] are prepared similarly to the suspensions of C<sub>60</sub>/IL. Picture of these samples is given in SI. All samples seem similar after the preparation at all tested concentrations: with C<sub>60</sub>F<sub>48</sub>, up to the concentration of 3 mg/mL, all samples are visually identical to a sample with neat IL. The contrast between the C<sub>60</sub> and C<sub>60</sub>F<sub>48</sub> samples is impressive: while with 0.30 mg/mL of C<sub>60</sub> in [BmIm][NTf<sub>2</sub>] the sample is completely opaque, with 3 mg/mL of C<sub>60</sub>F<sub>48</sub> the sample is completely transparent. Expectedly, all samples with C<sub>60</sub>F<sub>48</sub> keep their visual characteristic with time: after 6 weeks all samples are still transparent and no sedimentation was observed with the naked eye (pictures of clear samples after preparation and after 6 weeks are given in SI).

While it is not possible to observe the presence of C<sub>60</sub>F<sub>48</sub> in IL with the naked eye, agglomerates are visible with the help of an optical microscope. Picture of the bottom of sample for concentration up to 3 mg/mL of C<sub>60</sub>F<sub>48</sub> in [BmIm][NTf<sub>2</sub>] after 6 weeks of

sedimentation are shown in Fig 5. The presence of  $C_{60}F_{48}$  agglomerates is observable only for concentrations higher than 1.0 mg/mL while for  $C_{60}$  even at concentrations as low as 0.01 mg/mL the presence of agglomerates was identified. Naturally, particles observed with 1.5 mg/mL of  $C_{60}F_{48}$  represent a much higher proportion of the image than the few particles observed with  $C_{60}$  at a much lower concentration. The particles observed are around 10  $\mu\text{m}$  and most of the surface is not covered by them. With the concentration of 1.5 mg/mL of  $C_{60}F_{48}$ , if none of the powder was dispersed in the liquid and all material agglomerated on the bottom of the vial, all images should display a layer of thickness higher than 10  $\mu\text{m}$ . Most of the  $C_{60}F_{48}$  should then still be dispersed in the liquid phase. Moreover, no coloration could be observed in the case of  $C_{60}F_{48}$ , unlike in the case of  $C_{60}$  which induces a yellowish coloration with concentrations higher than 0.05 mg/mL.

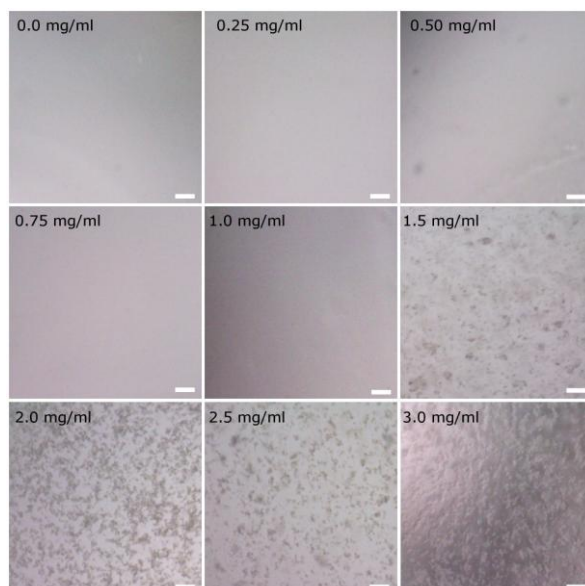


**Fig. 5.** Pictures of samples containing different concentrations of  $C_{60}F_{48}$  in  $[\text{BmIm}][\text{NTf}_2]$  after 6 weeks of sedimentation (0.0 mg/mL; 0.25 mg/mL; 0.50 mg/mL; 0.75 mg/mL; 1.0 mg/mL; 1.5 mg/mL; 2.0 mg/mL; 2.5 mg/mL; and 3.0 mg/mL). Scale bar: 100  $\mu\text{m}$ .

Observations made with the naked eye and with an optical microscope on samples containing  $C_{60}$  and  $C_{60}F_{48}$  in  $[\text{BmIm}][\text{NTf}_2]$  are summarized in Table 1. The range of concentrations used for  $C_{60}$  is 10 times lower than for the  $C_{60}F_{48}$ . Despite using lower concentrations with  $C_{60}$ , agglomeration is more clearly observed than with the fluorinated  $C_{60}F_{48}$ . Agglomerates were found on the bottom of the vial using an optical microscope at all tested concentrations with  $C_{60}$  (down to 0.01 mg/mL) while with the  $C_{60}F_{48}$ , the agglomerates could only be observed for concentration higher than 1.0 mg/mL. Moreover, while the samples were left for 6 weeks the sedimentation was clearly observable for concentrations higher than 0.05 mg/mL of  $C_{60}$ , and the top part of the sample is becoming much clearer. On the other hand, for  $C_{60}F_{48}$ ,

sedimentation can only be observed with an optical microscope, and even after 6 weeks, the sedimentation cannot be observed with the naked eye, despite the much higher concentration of the material added. These observations lead to the conclusion that the  $C_{60}F_{48}$  has a higher affinity with the IL than the  $C_{60}$ .

**Table 1: Visual observation of  $C_{60}$  and  $C_{60}F_{48}$  in [BmIm][NTf<sub>2</sub>].**

$C_{60}$	<b>Weight (mg/mL)</b>	<b>0</b>	<b>0.01</b>	<b>0.025</b>	<b>0.05</b>	<b>0.10</b>	<b>0.15</b>	<b>0.20</b>	<b>0.30</b>
	<b>Molar concentration (mmol/L)</b>	0	0.014	0.03	0.07	0.14	0.21	0.28	0.42
	<i>Color</i> <sup>1</sup>	Clear	Clear	Clear	Yellow	Yellow	Yellow	Yellow	Yellow
	<i>Sedimentation</i> <sup>2</sup>	No	Yes	Yes	Yes	Yes	Yes	Yes	Yes
$C_{60}F_{48}$	<b>Weight (mg/mL)</b>	<b>0</b>	<b>0.25</b>	<b>0.50</b>	<b>1.0</b>	<b>1.5</b>	<b>2.0</b>	<b>2.5</b>	<b>3.0</b>
	<b>Molar concentration (mmol/L)</b>	0	0.15	0.31	0.61	0.92	1.23	1.53	1.84
	<i>Color</i> <sup>1</sup>	Clear	Clear	Clear	Clear	Clear	Clear	Clear	Clear
	<i>Sedimentation</i> <sup>2</sup>	No	No	No	No	Yes	Yes	Yes	Yes

<sup>1</sup>: Color corresponds to the supernatant liquid phase after 6 weeks of sedimentation. <sup>2</sup>: Sedimentation is the observation using a microscope looking at the bottom face of the sample.

### 3.4 Optical Spectroscopy

UV-vis spectra of the samples containing  $C_{60}$  and  $C_{60}F_{48}$  in the IL were taken repeatedly to obtain a more precise observation of the agglomeration/sedimentation of over 6 weeks. Each spectrum is taken at around 1 cm from the top of the liquid phase while the liquids phases are systematically around 3 cm high. Spectra of the lowest concentrations (i.e. without saturated spectrum) are given in Fig.6 after around 1 hour and after 6 weeks. In the case of  $C_{60}$ , the UV-vis spectra are saturated with absorbance higher than 3.5 at 400 nm for concentrations higher than 0.10 mg/mL. The evolution of the spectra during this time is continuous and spectra taken at other times are given in SI. After 4 weeks none of the spectra are saturating, which illustrates the slow sedimentation of the  $C_{60}$  in the IL. The slow sedimentation could be at least partially explained by the viscosity of the dry IL: around 60 mPa.s at 20°C for [BmIm][NTf<sub>2</sub>] [31]. Spectra for the lowest concentrations (0.01 and 0.025 mg/mL) do not change significantly during the 6 weeks of the experiment, unlike the spectra obtained from the sample with higher concentrations of  $C_{60}$  ( $\geq 0.05$  mg/mL). For these higher concentrations, intensities of the UV-vis spectra are decreasing with time which should correspond to the sedimentation of the particles. This hypothesis is confirmed by the observation of particles on

the bottom of the cuvette containing the higher amount of  $C_{60}$  and the color of the solution which became brighter; as observable in Fig.4.

The two peaks observed in Fig.6 at 265 and 328 nm are comparable to those observed in n-alkanes [32]. Moreover, the increase of the signal at a higher wavelength (450 nm) could be assigned to the agglomeration of  $C_{60}$ , and the ratio of absorbances at 330 and 450 nm is considered as an indication of the degree of aggregation of  $C_{60}$  [33]. This ratio is decreasing when the concentration increases above 0.025 mg/mL. For concentration  $\leq 0.025$  mg/mL, the  $C_{60}$  does not show any sedimentation over 6 weeks, we could then estimate that most of the  $C_{60}$  is solubilized in [BmIm][NTf<sub>2</sub>] up to 0.025 mg/mL. This conclusion is comparable with the conclusions realized on  $C_{60}$  in comparable imidazolium NTf<sub>2</sub> based ILs in the literature using UV-vis spectroscopy [34, 35].

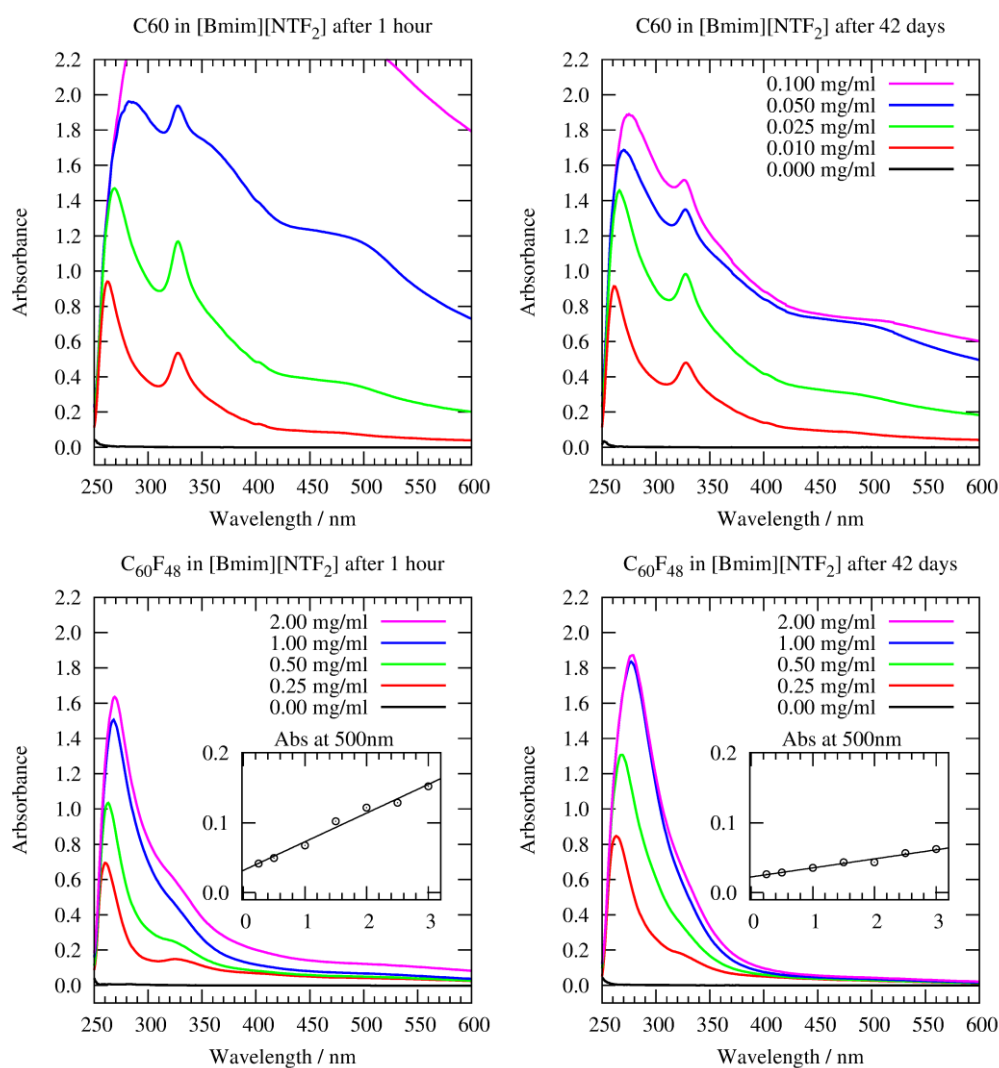


**Fig. 6.** Comparison of UV-vis spectra of  $C_{60}$  and  $C_{60}F_{48}$  in [BmIm][NTf<sub>2</sub>] at different concentrations after 1 hour and 6 weeks. The spectrum of the IL was used as background. For the figure on the  $C_{60}F_{48}$ , an insert has been added to visualize the evolution of the intensity at 500 nm as the function of the quantity (in mg/mL) of  $C_{60}F_{48}$ .



UV-vis spectra of  $C_{60}F_{48}$  in [BmIm][NTf<sub>2</sub>] over a range of concentration between 0.25 and 3.0 mg/mL were recorded during 6 weeks. Following the visual observations, visible light is almost not absorbed by any sample neither after 1 hour nor after 6 weeks. However, at the beginning of the experiment in the range between 350 and 600 nm, the absorbance is increasing slightly with the concentration of  $C_{60}F_{48}$ , as shown in the inserts of Fig.6. The signal rises to an absorbance of 0.15 at 500 nm for the concentration of 3.0 mg/mL of  $C_{60}F_{48}$ . At this wavelength, the absorbance increases linearly for concentrations from 0.25 to 3.0 mg/mL. At a lower wavelength, the main signal is at 260 nm with the concentration of 0.25 mg/mL and shifts continuously to 274 nm with the concentration of 3.0 mg/mL. Moreover, a shoulder at around 325 nm is also observable. While the band at around 260 nm is increasing with time, the baseline (500 nm) and the shoulder at 325 nm are both decreasing with time. If like in the case of  $C_{60}$ , the signal at a higher wavelength corresponds to agglomeration and the band at around 260 nm is assigned to the monomer, the observation might indicate a slow separation of agglomerates into monomers. However, all these fluctuations are rather modest and no clear sedimentation or aggregation of  $C_{60}F_{48}$  could be observed with the naked eye in [BmIm][NTf<sub>2</sub>].

The absence of micrometric particles is confirmed by the absence of scattering of the light when a laser with visible light was passing through the samples, unlike in the case of  $C_{60}$  at much lower concentrations (0.10 mg/mL). Fig.7 is illustrating the presence and absence of scattering light with a red laser (wavelength around 650 nm). While the laser is passing the sample containing initially 0.10 mg/mL of  $C_{60}$ , part of the light is scattered by the largest particles which are still present in the supernatant phase (after 3 months of sedimentation). The sample with 3.0 mg/mL of  $C_{60}F_{48}$  is almost not showing any scattering: most of the red light observed for both  $C_{60}F_{48}$  in IL and neat IL are coming from the interfaces of the UV-vis cuvettes. However, the small scattering is observed in the case of  $C_{60}F_{48}$ , and it is coherent with the baseline of UV-vis spectra (measured at 500 nm in Fig. 6) which is increasing with the concentration of  $C_{60}F_{48}$  in IL and decreasing with time. The decrease of the intensity at 500 nm could therefore be assigned either to the slow sedimentation of the small amount of the larger aggregates of  $C_{60}F_{48}$  in IL or to slow disaggregation of particles which could be coherent with the increase of the band at around 260 nm with time.

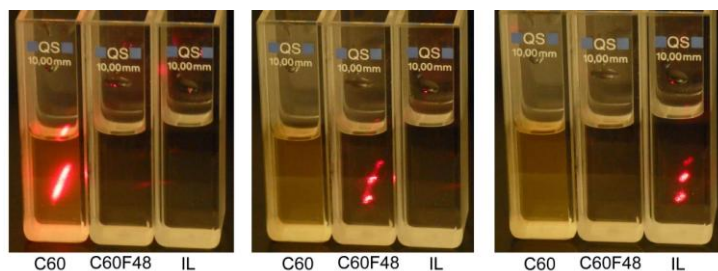


**Fig.7.** Pictures of 3 UV-vis cuvettes containing the supernatant phase of  $C_{60}$  in IL (0.10 mg/mL),  $C_{60}F_{48}$  in IL (3.0 mg/mL) and the neat [BmIm][NTf<sub>2</sub>]. From left to right the laser is pointing respectively to  $C_{60}$  (left),  $C_{60}F_{48}$  (center) and the neat IL (right).

Considering the amount of scattering of the laser light with only 0.10 mg/mL of  $C_{60}$  and the much smaller amount of scattering with 3.0 mg/mL of  $C_{60}F_{48}$ , the number of large objects present in the IL is most probably rather modest in the case of fluorinated fullerenes. Since we also observed insignificant sedimentation with the sample containing  $C_{60}F_{48}$ , we can conclude that fluorinated fullerenes are well solubilized in [BmIm][NTf<sub>2</sub>] even at a concentration as high as 1.0 mg/mL.

## Conclusion

The main objective of this work was to contribute to the understanding of the impact of fluorination of carbon nanomaterials in ionic liquids (ILs) based on the fluorinated [NTF<sub>2</sub>] anion. Spherical  $C_{60}$  and  $C_{60}F_{48}$  were used as a model. The presence of fluorine atoms on fullerene enhances the stability of solvated molecules in IL thanks to the limitation of the aggregation of  $C_{60}F_{48}$  in [BmIm][NTf<sub>2</sub>]. The change of the carbon hybridization from  $sp^2$  to  $sp^3$  through the formation of covalent C-F bonds suppresses the  $\pi$ - $\pi$  interaction between molecules. Moreover, electrostatic repulsion between fluorine atoms hinders the re-agglomeration. On the contrary in the case of  $C_{60}$ , van der Waals interaction favors the aggregation. Fluorination appears then as an efficient way to avoid the use of volatile organic solvents (used as co-solvent to enhance the dispersion mechanism). This route may be useful for other carbonaceous nanomaterials, i.e. unbundling of fluorinated nanotubes and preparation using exfoliation of fluorinated graphene and F-diamane. The enhanced fluorinated nanocarbon/IL interactions would favor both the exfoliation and unbundling and the use of mild conditions for exfoliation/unbundling, i.e. sonication with low power for a short time, that avoid partial defluorination.

The stabilized concentrations, that involved residual aggregates, small clusters and solvated molecules, are less than 0.05 mg/mL (0.07 mmol/L) and more than 1.0 mg/mL (or 0.61 mmol/L) for C<sub>60</sub> and C<sub>60</sub>F<sub>48</sub>, respectively. Regarding the interactions between ionic media and C<sub>60</sub>F<sub>48</sub>, the mobility of the  $\pi$ -electrons is decreased during the fluorination. Consequently, the polarization effects on the interactions with charged or polar species are weakened and  $\pi$ - $\pi$  stacking, which is responsible for the strong cohesion between carbonaceous nanomaterials, is decreased favoring solvation. The fluorination has therefore a considerable impact on the ability of the fluorinated IL to solubilized fluorinated nanomaterials. In [BmIm][NTf<sub>2</sub>], C<sub>60</sub>F<sub>48</sub> exists rather as solvated isolated molecules or small clusters whereas raw C<sub>60</sub> tends to form large aggregates.

#### **Acknowledgments:**

The authors would like to thank ANR (French National Agency for Research) for the financial support of the CLINT project.

## References

- [1] S. Nath, H. Pal, A.V. Sapre, Effect of solvent polarity on the aggregation of fullerenes: a comparison between C<sub>60</sub> and C<sub>70</sub>, *Chem. Phys. Lett.*, 360 (2002) 422-428.
- [2] V.V. Chaban, C. Maciel, E.E. Fileti, Does the Like Dissolves Like Rule Hold for Fullerene and Ionic Liquids?, *J Solution Chem.* 43 (2014) 1019-1031.
- [3] V.V. Chaban, C. Maciel, E.E. Fileti, Solvent Polarity Considerations Are Unable to Describe Fullerene Solvation Behavior, *J. Phys. Chem. B.* 118 (2014) 3378-3384.
- [4] E.E. Fileti, V.V. Chaban, Imidazolium Ionic Liquid Helps to Disperse Fullerenes in Water, *J. Phys. Chem. Lett.* 5 (2014) 1795-1800.
- [5] E.E. Fileti, V.V. Chaban, Structure and Supersaturation of Highly Concentrated Solutions of Buckyball in 1-Butyl-3-Methylimidazolium Tetrafluoroborate, *J. Phys. Chem. B.* 118 (2014) 7376-7382.
- [6] C. Maciel, E.E. Fileti, R. Rivelino, Note on the Free Energy of Transfer of Fullerene C<sub>60</sub> Simulated by Using Classical Potentials, *J. Phys. Chem. B.* 113 (2009) 7045-7048.
- [7] B. Han, M.N. Karim, Cytotoxicity of Aggregated Fullerene C<sub>60</sub> Particles on CHO and MDCK Cells, *Scanning.* 30 (2008) 213-220.
- [8] R. Pamies, M.D. Aviles Gonzalez, J. Arias-Pardilla, T. Espinosa, F. Vilches, J. Sanes, M.D. Bermúdez, Antiwear performance of ionic liquid+graphene dispersions with anomalous viscosity-temperature behavior, *Tribol. Int.* 122 (2018).
- [9] R.S. Ruoff, D.S. Tse, R. Malhotra, D.C. Lorents, Solubility of fullerene (C<sub>60</sub>) in a variety of solvents, *J. Phys. Chem.* 97 (1993) 3379-3383.
- [10] K. Semenov, N. Charykov, V. Keskinov, A. Piartman, A. Blokhin, A. Kopyrin, Solubility of Light Fullerenes in Organic Solvents, *J. Chem. Eng. Data.* 55 (2009).
- [11] D.V. Konarev, R.N. Lyubovskaya, N.y.V. Drichko, E.I. Yudanov, Y.M. Shul'ga, A.L. Litvinov, V.N. Semkin, B.P. Tarasov, Donor-acceptor complexes of fullerene C<sub>60</sub> with organic and organometallic donors, *J. Matter. Chem.* 10 (2000) 803-818.
- [12] S. Talukdar, P. Pradhan, A. Banerji, Electron Donor-Acceptor Interactions of C<sub>60</sub> with  $\sigma$ - and  $\pi$ -Donors: A Rational Approach Towards its Solubility, *Fullerene Sci. Technol.* 5 (1997) 547-557.
- [13] J.H. Holloway, E.G. Hope, R. Taylor, G.J. Langley, A.G. Avent, T.J. Dennis, J.P. Hare, H.W. Kroto, D.R.M. Walton, Fluorination of buckminsterfullerene, *J. Chem. Soc. Chem. Commun.* (1991) 966-969.
- [14] V.V. Chaban, E.E. Fileti, Strong electronic polarization of the C<sub>60</sub> fullerene by imidazolium-based ionic liquids: accurate insights from Born-Oppenheimer molecular dynamic simulations, *PCCP.* 17 (2015) 15739-15745.
- [15] V.V. Chaban, E.E. Fileti, Which fullerenols are water soluble? Systematic atomistic investigation, *New J. Chem.* 41 (2017) 184-189.
- [16] J. Hallett, T. Welton, Room-Temperature Ionic Liquids: Solvents for Synthesis and Catalysis. 2, *Chem. Rev.* 111 (2011) 3508-3576.
- [17] O.V. Boltalina, A.a.K. Abdul-Sada, R. Taylor, Hyperfluorination of [60]fullerene by krypton difluoride, *J. Chem. Soc., Perkin Trans. 2,* (1995) 981-985.
- [18] O.V. Boltalina, A.Y. Lukonin, V.K. Pavlovich, L.N. Sidorov, R. Taylor, A.K. Abdul-Sada, Reaction of [60]Fullerene with Terbium(IV) Fluoride, *Fullerene Sci. Technol.* 6 (1998) 469-479.
- [19] O.g. V. Boltalina, N. A. Galeva, Direct fluorination of fullerenes, *Russ. Chem. Rev.* 69 (2000) 609-621.
- [20] O.V. Boltalina, Fluorination of fullerenes and their derivatives, *J. Fluorine Chem.* 101 (2000) 273-278.

- [21] O.V. Boltalina, A.D. Darwish, J.M. Street, R. Taylor, X.-W. Wei, Isolation and characterisation of C<sub>60</sub>F<sub>4</sub>, C<sub>60</sub>F<sub>6</sub>, C<sub>60</sub>F<sub>8</sub>, C<sub>60</sub>F<sub>7</sub>CF<sub>3</sub> and C<sub>60</sub>F<sub>2</sub>O, the smallest oxahomofullerene; the mechanism of fluorine addition to fullerenes, *J. Chem. Soc. Perkin Trans. 2*, (2002) 251-256.
- [22] O. Boltalina, V. Markov, P. Troshin, A. Darwish, J. Street, R. Dr, C<sub>60</sub>F<sub>20</sub>: “Saturnene”, an Extraordinary Squashed Fullerene, *Angew. Chem.* 113 (2001) 809-811.
- [23] W. Zhang, M. Dubois, K. Guerin, P. Bonnet, H. Kharbache, F. Masin, A.P. Kharitonov, A. Hamwi, Effect of curvature on C-F bonding in fluorinated carbons: from fullerene and derivatives to graphite, *PCCP*, 12 (2010) 1388-1398.
- [24] S. Kawasaki, T. Aketa, H. Touhara, F. Okino, O.V. Boltalina, I.V. Gol'd, S.I. Troyanov, R. Taylor, Crystal Structures of the Fluorinated Fullerenes C<sub>60</sub>F<sub>36</sub> and C<sub>60</sub>F<sub>48</sub>, *J. Phys. Chem. B.* , 103 (1999) 1223-1225.
- [25] Y. Sato, K. Itoh, R. Hagiwara, T. Fukunaga, Y. Ito, On the so-called “semi-ionic” C–F bond character in fluorine–GIC, *Carbon*, 42 (2004) 3243-3249.
- [26] T. Mallouk, B.L. Hawkins, M.P. Conrad, K. Zilm, G.E. Maciel, N. Bartlett, Raman, Infrared and n.m.r. Studies of the Graphite Hydrofluorides, *Philos. Trans. Royal Soc. A.* 314 (1985) 179-187.
- [27] Panich AM, Nuclear magnetic resonance study of fluorine–graphite intercalation compounds and graphite fluorides, *Synth.Met.* 100 (1999) 169-185.
- [28] J. Giraudet, M. Dubois, K. Guérin, C. Delabarre, A. Hamwi, F. Masin, Solid-State NMR Study of the Post-Fluorination of (C<sub>2.5</sub>F)<sub>n</sub> Fluorine–GIC, *J. Phys. Chem. B.* 111 (2007) 14143-14151.
- [29] M. Dubois, J. Giraudet, K. Guérin, A. Hamwi, Z. Fawal, P. Pirotte, F. Masin, EPR and Solid-State NMR Studies of Poly(dicarbon monofluoride) (C<sub>2</sub>F)<sub>n</sub>, *J. Phys. Chem. B.* 110 (2006) 11800-11808.
- [30] J. Giraudet, M. Dubois, K. Guérin, JP Pinheiro, A. Hamwi, WEE Stone, P. Pirotte, F. Masin, Solid-state F-19 and C-13 NMR of room temperature fluorinated graphite and samples thermally treated under fluorine: Low-field and high-resolution studies, *J. Solid State Chem.* 178 (2005) 1262-1268.
- [31] J. Jacquemin, P. Husson, A.A.H. Padua, V. Majer, Density and viscosity of several pure and water-saturated ionic liquids, *Green Chem.* 8 (2006) 172-180.
- [32] I. Renge, Solvent Effects on the Absorption Maxima of Fullerenes C<sub>60</sub> and C<sub>70</sub>, *J. Phys. Chem.* 99 (1995) 15955-15962.
- [33] R.V. Bensasson, E. Bienvenue, M. Dellinger, S. Leach, P. Seta, C<sub>60</sub> in Model Biological Systems. A Visible-UV Absorption Study of Solvent-Dependent Parameters and Solute Aggregation, *J. Phys. Chem.* 98 (1994) 3492-3500.
- [34] J. Szala-Bilnik, M.F. Costa Gomes, A.A.H. Pádua, Solvation of C<sub>60</sub> Fullerene and C<sub>60</sub>F<sub>48</sub> Fluorinated Fullerene in Molecular and Ionic Liquids, *J. Phys. Chem. C.* 120 (2016) 19396-19408.
- [35] H. Liu, G.-h. Tao, D.G. Evans, Y. Kou, Solubility of C<sub>60</sub> in ionic liquids, *Carbon.* 43 (2005) 1782-1785.